



Effects of reactant composition and nonuniformities on temperature fronts

J. Annamalai, C. Ballandis, M. Soman, M. A. Liauw, and D. Luss

Citation: [The Journal of Chemical Physics](#) **107**, 1896 (1997); doi: [10.1063/1.474540](https://doi.org/10.1063/1.474540)

View online: <http://dx.doi.org/10.1063/1.474540>

View Table of Contents: <http://scitation.aip.org/content/aip/journal/jcp/107/6?ver=pdfcov>

Published by the [AIP Publishing](#)

Articles you may be interested in

[The internal energy of CO₂ produced by the catalytic oxidation of CH₃OH by O₂ on polycrystalline platinum](#)
J. Chem. Phys. **131**, 154701 (2009); [10.1063/1.3249685](https://doi.org/10.1063/1.3249685)

[Chemical diffusion of CO in mixed CO + O adlayers and reaction-front propagation in CO oxidation on Pd\(100\)](#)
J. Chem. Phys. **125**, 054709 (2006); [10.1063/1.2221690](https://doi.org/10.1063/1.2221690)

[The catalytic role of water in CO oxidation](#)
J. Chem. Phys. **119**, 6324 (2003); [10.1063/1.1602053](https://doi.org/10.1063/1.1602053)

[Stochastic model of reaction rate oscillations in the CO oxidation on nm-sized palladium particles](#)
J. Chem. Phys. **116**, 2098 (2002); [10.1063/1.1429234](https://doi.org/10.1063/1.1429234)

[Mathematical modeling of complex oscillatory phenomena during CO oxidation over Pd zeolite catalysts](#)
J. Chem. Phys. **111**, 8105 (1999); [10.1063/1.480144](https://doi.org/10.1063/1.480144)



Effects of reactant composition and nonuniformities on temperature fronts

J. Annamalai, C. Balladis,^{a)} M. Soman, M. A. Liauw,^{b)} and D. Luss^{c)}

Department of Chemical Engineering, University of Houston, Houston, Texas 77204-4792

(Received 29 January 1997; accepted 8 May 1997)

Stationary and spatially oscillating temperature fronts separating regions with high and low temperatures (amplitudes up to 120 K) formed during the atmospheric oxidation of carbon monoxide on a Pd on alumina ring kept in a mixed reactor. The sharp fronts bounded either one or two low temperature regions. The transition from stationary to spatially oscillating fronts occurred at a feed CO/O₂ concentration ratio close to 2.0 and was independent of the reactor temperature. The net rate of local heat generation on the ring was nonuniform leading to angular variation of the temperature of the ignited state. Front motions were affected by both the nonuniformity of the system and the interaction between the catalyst and the ambient gas. The two fronts bounding a low temperature region usually moved at different velocities and their velocities increased with increasing oxygen concentration. In most cases the two fronts did not move in phase, but sometimes they moved in tandem generating a back-and-forth pulse motion. The spatial amplitude of the oscillations decreased as the slope of the net heat generation activity became steeper. The spatial variation of the standard deviation of the temperature was helpful in assessing the dynamics of the oscillating fronts. © 1997 American Institute of Physics. [S0021-9606(97)53230-2]

I. INTRODUCTION

The formation and stabilization of spatiotemporal patterns has been studied in a large number of physical, chemical, and living systems. The interaction between diffusion and chemical reactions may be used to explain and predict many of these observations.¹ Temperature and concentration patterns observed in atmospheric catalytic systems are affected, in addition, by global coupling as well as intrinsic and evolving system nonuniformities. Global coupling generated by the interaction among the catalytic surface elements and the mixed ambient fluid² introduces a new mode of communication among the surface elements. In some cases, it stabilizes pattern formation (such as when a positive-order reaction occurs in a constant temperature CSTR), while in others it may synchronize the various surface elements (such as when a highly exothermic reaction is carried out in an adiabatic reactor). In addition, nonuniformities in either the catalytic activity and/or the transport coefficients (hereafter referred to as “nonuniformity”) may strongly affect pattern evolution and stabilization and lead to a novel, rich, and intricate set of patterns which would not exist in their absence. The first report of nonuniform temperature on a catalytic wire due to nonuniformities was by Davies³ in 1935. Temperature patterns which were affected by nonuniformities have been observed on electrically heated wires,^{4,5} metal catalysts,^{6–8} and supported catalysts.⁹ Fascinating concentration patterns have been observed in ultra-high vacuum experiments.¹⁰ Intricate patterns are observed when the nature of the local dynamics changes along the

surface, so that, e.g., fronts can propagate only on part of the surface and cannot penetrate into certain surface regions.

Several theoretical studies of nonuniformities have been reported recently.^{11–21} Analyses using the Fitzhugh–Nagumo kinetic model suggest that the front motion is strongly affected by the magnitude, length scale, and slope of the non-uniform activity. Experiments checking some of these predictions were carried out for a well-defined electrical system.¹² Unfortunately, in heterogeneous catalytic systems it is usually not possible to determine the exact catalytic activity and transport coefficients profile (hereafter referred to as the “activity profile”) and the experiments are further masked by global coupling. It has been suggested that the main features of the underlying nonuniformity may be discerned from the observed pattern by evaluation of the front velocity¹² or the time-averaged activator profile.¹⁶ Both methods yield useful results only if the fronts move through all the points on the surface, as is the case for a rotating pulse on a ring-shaped catalyst. One of our goals was to examine if, how, and what information may be gained about the non-uniformity by inspection of the patterns.

Hagberg *et al.*¹⁷ predicted that an Ising–Bloch bifurcation²² from stationary to oscillatory front can be obtained in a nonuniform bistable system. This transition was observed in a variety of uniform physical and chemical systems, such as coupled electrical oscillators,²³ ferrocyanide–iodate–sulphite reaction,²⁴ and CO oxidation on a Pt single crystal at low pressures.¹³ One of our goals was to find such a transition for an atmospheric catalytic reaction conducted on a nonuniform surface.

II. EXPERIMENTAL SYSTEM AND PROCEDURE

The experiments were conducted on a thin catalytic ring of Pd supported on γ alumina. It was prepared by pressing (2 tons/cm²) a palladium-on-alumina powder (1% Pd; Ald-

^{a)}Permanent address: Institut für Angewandte und Physikalische Chemie, Universität Bremen, Bibliothekstrasse, D-28334 Bremen, Germany.

^{b)}Present address: Lehrstuhl für Technische Chemie I, Friedrich-Alexander Universität Erlangen-Nürnberg, Egerlandstrasse 3, D-91058 Erlangen, Germany.

^{c)}Author to whom correspondence should be addressed.

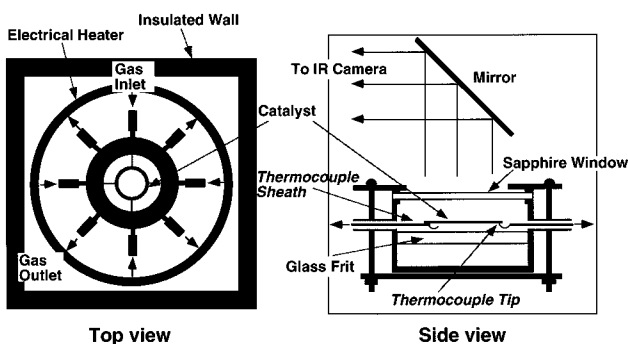


FIG. 1. Schematic of the reactor. The catalytic ring (27 mm i.d., 34 mm o.d., and 0.9 mm thick) was placed in a cylindrical stainless steel reactor, 68 mm i.d. and 39 mm height. The reactor was placed inside an insulated oven and the reactor wall temperature controlled by a PID controller (Omega CN2041). The reactor lid was an infrared-transparent sapphire window (Union Carbide Crystals Division). The reactor was operated at atmospheric pressure. The gases were fed through four angularly symmetric inlet ports (2.4 mm i.d.) located near the bottom of the reactor chamber, and the product gases exited through four similar outlet ports (4.7 mm i.d., shifted with respect to inlet ports by 45° and 13 mm upwards). A cylindrical glass frit (67 mm diam, 6 mm thickness, 150 μm average pore size) was placed between the catalyst and inlets to distribute the feed. The effluent carbon monoxide concentration was measured by an infrared analyzer (Anarad, AR-411).

rich) in a die. Details of catalyst preparation were reported by Soman.²⁵ The feed gases were prepurified grade nitrogen (purity 99.998%) and extra dry grade oxygen (purity 99.6%) in stainless steel cylinders and certified grade mixture of 30 vol % carbon monoxide and 70 vol % nitrogen in aluminum cylinders (Linde division of Union Carbide). Aluminum cylinders were used to avoid the formation of iron and nickel carbonyls which could deactivate the catalyst. The carbon monoxide was passed through an in-line carbonyl trap of a molecular sieve adsorbent (Linde, 5A zeolite) kept at 240 °C. The feed gases were mixed in a bed of glass beads, purified, and dried by in-line activated charcoal purifiers (Linde) before entering the reactor. Thermal mass flow controllers (Tylan FC-280 and FC-260, accuracy $\pm 1\%$) were used to control the oxygen, nitrogen, and carbon monoxide flow rates. The total flow rate was 800 sccm, which led to a residence time of about 6 s. No reaction was observed in the empty (without catalyst) reactor for temperatures up to 200 °C. Experiments repeated after several weeks were qualitatively but not quantitatively reproducible. This behavior is typical for heterogeneous catalysts.^{7,26,27}

An AGEMA (Thermovision 780) indium–antimonide (In–Sb) camera sensitive to 2–5.6 μm measured the temperature profile of the catalytic ring. A mirror was used to view the catalyst, as the camera had to be operated horizontally (Fig. 1, right-hand side). The camera scanned a 5.6 cm \times 4.6 cm field with a spatial resolution of 0.3 mm². The 128 \times 64 image matrix of local radiation levels (8 bit) was converted to local surface temperature images, digitized, and recorded on a Mac II computer for later analysis.

No temperature variations in the radial direction were observed, indicating that the system may be treated as one dimensional with periodic boundary conditions. Two-

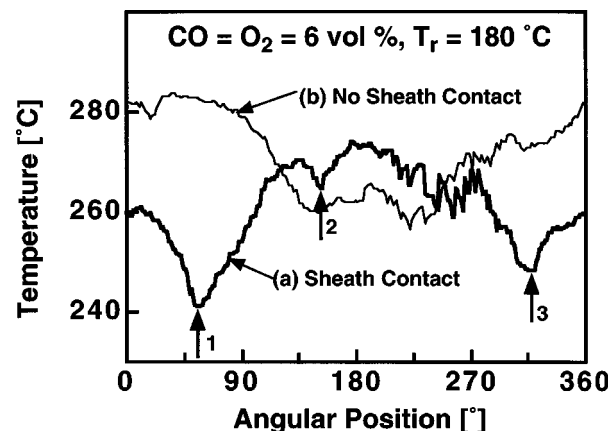


FIG. 2. Temperature profiles of the fully ignited catalyst indicating catalyst nonuniformity. (a) Thermocouple sheaths touching the catalyst (arrows indicate position of thermocouples). The local minima in the temperature profile (angular positions 55°, 155°, and 315°) coincided with the location of the three thermocouples touching the catalyst. $T_{\max} = 274\text{ }^{\circ}\text{C}$; $T_{\min} = 241\text{ }^{\circ}\text{C}$; $T_{\text{ave}} = 261\text{ }^{\circ}\text{C}$. (b) Catalyst supported at same locations on tips of the thermocouples. $T_{\max} = 284\text{ }^{\circ}\text{C}$; $T_{\min} = 257\text{ }^{\circ}\text{C}$; $T_{\text{ave}} = 272\text{ }^{\circ}\text{C}$.

dimensional maps of surface temperature as a function of time and angular position were constructed by placing a series of one-dimensional temperature images next to each other.

The catalyst was supported horizontally by three iron–constantan thermocouples (Omega) enclosed in stainless steel sheaths with about 1/2 in. of the wire outside the sheath. To introduce a nonuniformity in a defined manner, the catalytic ring was placed such that the sheaths of two of the three supporting thermocouples touched it (Fig. 1, right-hand side), thereby increasing the local heat loss.

III. EXPERIMENTAL RESULTS

The temperature profiles on a ring-shaped supported Pd catalyst were measured during the oxidation of carbon monoxide. Experiments by Liauw *et al.*²⁸ showed that this system exhibited bistability over a bounded region of composition and temperatures, i.e., either an ignited or extinguished state existed for the same operating conditions. In most of the experiments the feed contained 6 vol % CO. The feed oxygen concentrations were in the range of 2.4–12 vol % so that the feed CO/O₂ concentration ratio was between 0.5 and 2.5. In some experiments the feed contained 4 vol % CO.

The catalyst nonuniformities affected the net rate of local heat generation. The IR measurements revealed that the temperature of the fully ignited catalyst was not uniform. A typical case is shown in Fig. 2 for a feed containing 6 vol % CO and 6 vol % O₂ at a reactor temperature of 180 °C. When the catalytic ring did not touch the sheath of any of the three thermocouples the minimum and maximum surface temperatures differed by 27 °C, while the average ring temperature exceeded that of the ambient gas by 92 °C. As the ring temperature is nonuniform, we define a state to be fully ignited (extinguished) when all the points on the ring are on the ignited (extinguished) branch. The reaction rate on the ig-

nited branch was high and the average catalyst temperature was significantly higher than that of the reactor ($60\text{--}80^\circ\text{C}$ for a feed with 6 vol % CO). The reaction rate on the extinguished branch was negligible and the catalyst temperature was very close to that of the reactor.

In addition to the branches of fully extinguished and fully ignited states, a branch of nonuniform states existed, in which sharp stationary or oscillating temperature fronts separated the ignited and extinguished regions. A shift to this branch from the fully ignited branch was obtained by slowly decreasing the reactor temperature. As the reactor temperature was decreased, part of the catalyst extinguished, increasing the reactor CO concentration and leading to the formation of both high and low temperature regions. The temperature of the cold (hot) part was close to that of the extinguished (ignited) state for the same reactor concentration and temperature. The average reaction rate was always bounded between those of the fully ignited and extinguished states, so that the reactor CO concentration for a nonuniform state exceeded that of a fully ignited state for the same feed concentration. As the reaction rate and catalyst temperature increased monotonically with reactor CO concentration, the high temperature of a nonuniform state exceeded that of a fully ignited state for the same feed concentration, even though the reactor temperature was lower. Thus the amplitude of the temperature fronts of the nonuniform states increased with decreasing reactor temperature.

The extinguished regions tended to form around two locations (angular positions of 55° and 315°) at which local dips in the temperature of the fully ignited state were observed (Fig. 2). It was possible to obtain a low temperature region around either one of these locations by proper choice of the initial and operating conditions. Rotating the ring by 180° had minor influence on the temperature profile of a fully ignited state and on the nonuniform temperature patterns. This suggests that heat loss to the thermocouples and flow maldistribution were the major sources of the nonuniformities. Stationary temperature patterns were observed for a range of reactor temperatures for feed mixtures containing 6 vol % CO when oxygen was the limiting reactant, i.e., feed CO/O₂ concentration ratio was greater than or equal to 2. Typical stationary temperature fronts, which bound an extinguished region around the angular position of 315° , are shown in Fig. 3(a). Using different initial conditions these two temperature fronts could be placed around the 55° angular position. In both cases the temperature fronts were stationary and the effluent CO concentration was constant (within the instrumental noise).

The temperature fronts were also stationary for all reactor temperatures, but decreasing the reactor temperature increased the distance between them, i.e., the width of the low temperature region. For example, at 175°C the low temperature region occupied most of the ring, while the high temperature occupied only a small fraction of it [Fig. 3(b)]. The CO reactor concentration at 175°C (5.7 vol %) was higher than that at 199°C (5.3 vol %) due to the lower reaction rate. Consequently, the high temperature of the nonuniform state in a reactor kept at 175°C (260°C) exceeded that in a reac-

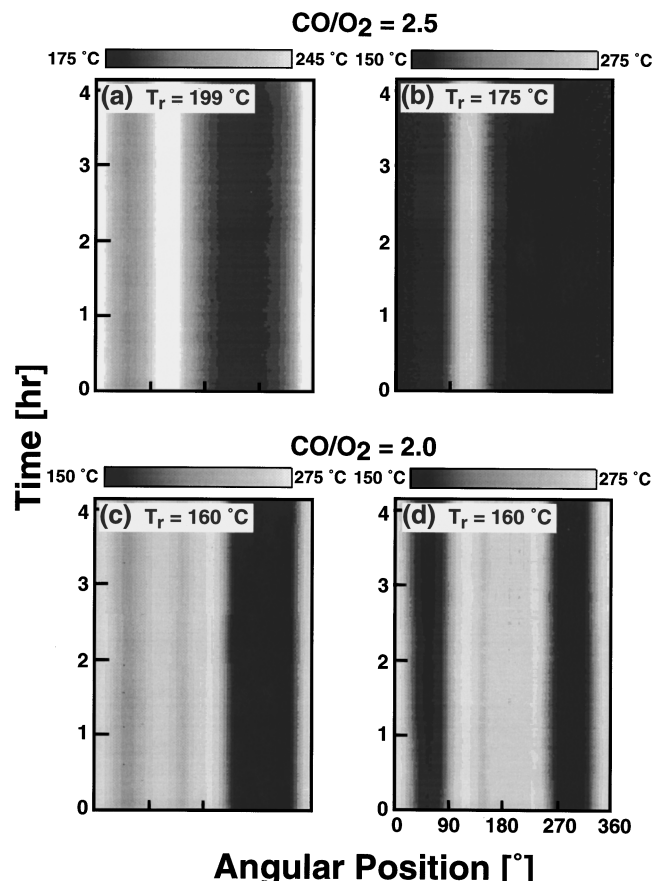


FIG. 3. The surface temperature as a function of time and angular position for stationary temperature fronts observed for feeds with 6 vol % CO and CO/O₂ concentration ratios of 2.5 and 2.0. The patterns in cases (c) and (d) were obtained for different initial conditions. The CO conversions were (a) 12.5%, (b) 4.5%, (c) 28.5%, and (d) 22.1%.

tor kept at 199°C (245°C). This observation is similar to that reported by Liauw *et al.*²⁸

Stationary temperature fronts were also obtained for a feed with a CO/O₂ concentration ratio of 2.0. Depending on the initial conditions, either one or two low temperature regions were obtained [Figs. 3(c) and 3(d)] for a reactor temperature of 160°C . When two low temperature regions [Fig. 3(d)] existed simultaneously, a smaller fraction of the ring was ignited and hence the effluent CO concentration (4.7 vol %) exceeded that when only one low temperature region [Fig. 3(c)] existed (4.3 vol %).

Either one or two pairs of back-and-forth moving temperature fronts were obtained for feed mixtures with feed CO/O₂ concentration ratios smaller than or equal to 1.9, i.e., mixtures in which CO was the limiting reactant. The low temperature regions were centered around 55° and/or 315° and the initial conditions determined which of the two states was obtained. Figures 4(a) and 4(b) describe a single low temperature region obtained at either one of these two locations with a reactor temperature of 140°C .

While the location of the fronts depended on the reactor temperature the nature of the oscillatory motion (spatial amplitude, frequency, and velocity) of the fronts was strongly

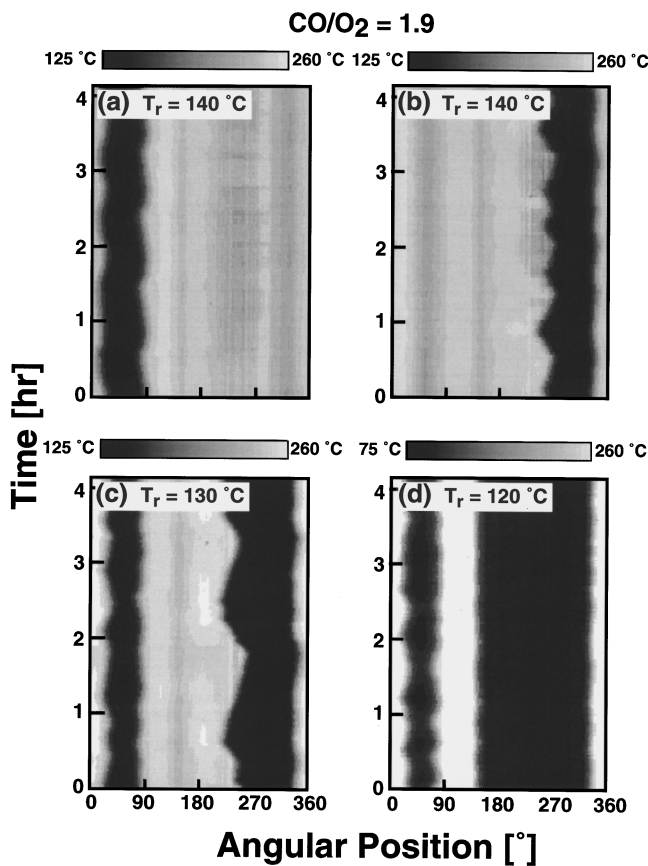


FIG. 4. The surface temperature as a function of time and angular position for spatially oscillating temperature fronts observed for feeds with 6 vol % CO and CO/O₂ concentration ratio of 1.9. Note the back-and-forth motion of the low temperature pulse in case (a) and the breathing motion in case (d). The difference between the patterns in cases (a) and (b) is due to different initial conditions. The CO conversions were (a) 32.3%, (b) 36.4%, (c) 27.6%, and (d) 17.0%.

dependent on their location on the ring and to a lesser degree on the reactor temperature. At a reactor temperature of 140 °C the fronts centered around 55° [Fig. 4(a)] oscillated back-and-forth in tandem tending to maintain a constant distance (1.7 mm) between themselves. They reversed their direction at about the same time, so that when one was an ignition front (its motion leads to local ignition), the second was an extinction front. The velocity of the front of the left-hand boundary was essentially independent of the direction (0.15 mm/min). However, on the right-hand boundary, the extinction front velocity (0.2 mm/min) exceeded that of the ignition front (0.1 mm/min). At lower reactor temperatures [Figs. 4(c) and 4(d)], the fronts bounding the low temperature region around 55° did not move in tandem. The extinction fronts usually moved at higher velocity (0.2–0.3 mm/min) than the ignition fronts (0.07–0.2 mm/min). The fronts on the left-hand boundary oscillated with a slightly higher spatial amplitude than those on the right-hand boundary. The amplitude of the spatial oscillations of the front on the left-hand side of the cold region around 315° in Figs. 4(b) and 4(c) was much larger than those of the other fronts. The velocities of the extinction and ignition fronts at 240° of the case shown in Fig. 4(c) were 0.3–0.4 and 0.2–0.3 mm/min,

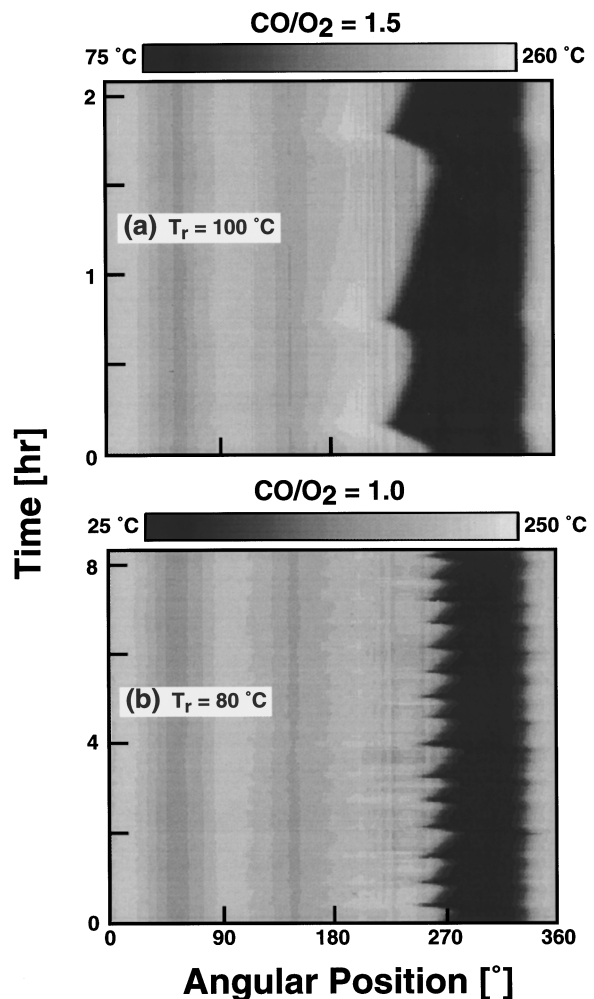


FIG. 5. The surface temperature as a function of time and angular position for spatially oscillating temperature fronts observed for feeds with 6 vol % CO and CO/O₂ concentration ratios of 1.5 and 1.0. The CO conversions were (a) 38.2% and (b) 36.7%.

respectively. Decreasing the reactor temperature from 130 to 120 °C shifted the left-hand boundary of the low temperature region from around 240° to 160° and decreased significantly the spatial amplitude and velocity of that front [Fig. 4(d)]. The amplitudes of the effluent CO concentration oscillations were 4%, 7%, 6%, and 5% of the feed concentration for the cases shown in Figs. 4(a)–4(d), respectively.

Qualitatively similar behavior was observed for higher oxygen feed concentrations i.e., lower feed CO/O₂ concentration ratios. Figures 5(a) and 5(b) illustrate the behavior for feed CO/O₂ concentration ratios of 1.5 and 1.0, respectively. Again, the oscillatory features of the fronts depended on their location on the ring. For example, the front on the left-hand boundary of the low temperature region at 315° oscillated with a higher spatial amplitude than that on the right-hand side. The extinction fronts moved faster (1 mm/min) than the ignition fronts (0.22 mm/min) and the transition from extinction to ignition fronts was sharp. The frequency of the oscillations increased with increasing oxygen concentration or decreasing feed CO/O₂ concentration ratio. For example, decreasing the feed CO/O₂ concentration ratio from

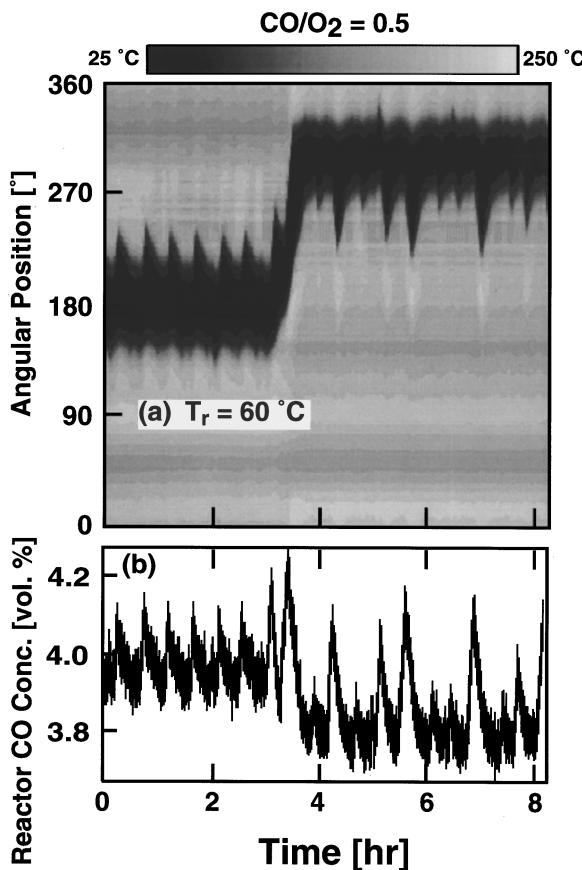


FIG. 6. A case in which the low temperature region shifted from around 180° to the preferred location around 315° . (a) The surface temperature as a function of time and angular position. (b) The corresponding temporal effluent CO concentration (average CO conversion—34.9%). The velocities of the ignition and extinction fronts around 180° (300°) were about 0.4 (0.7) mm/min and 1.5 (1.5–2.0) mm/min, respectively.

1.5 to 1.0 (Fig. 5) decreased the oscillations period from 45 to 30 min. The front velocity increased, in general, with increasing oxygen concentration. It was about 0.1–0.4 mm/min for a feed CO/O_2 concentration ratio of 1.9 and 1.0–2.5 mm/min for CO/O_2 concentration ratio of 0.5.

In one experiment, described by Fig. 6, the low temperature region formed initially around 180° rather than around 55° or 315° . However, after about 3.5 h it moved and then stayed around 315° . The oscillatory features of the fronts were strongly dependent on their location on the ring. For both cases, the fronts located between 200° and 270° oscillated with a much higher spatial amplitude than the fronts located around 150° and 325° . The amplitude of the spatial oscillations of the front located between 200° and 270° was rather constant when the cold pulse was centered at 180° . However, the amplitude became time dependent when the pulse was centered around 300° . The velocity of the extinction fronts at either location exceeded that of the ignition fronts.

In all our experiments with 6 vol % CO, the nature of the front movements (stationary or oscillatory) depended on the feed CO/O_2 concentration ratio, but not on the reactor temperature. However, the width of the low temperature re-

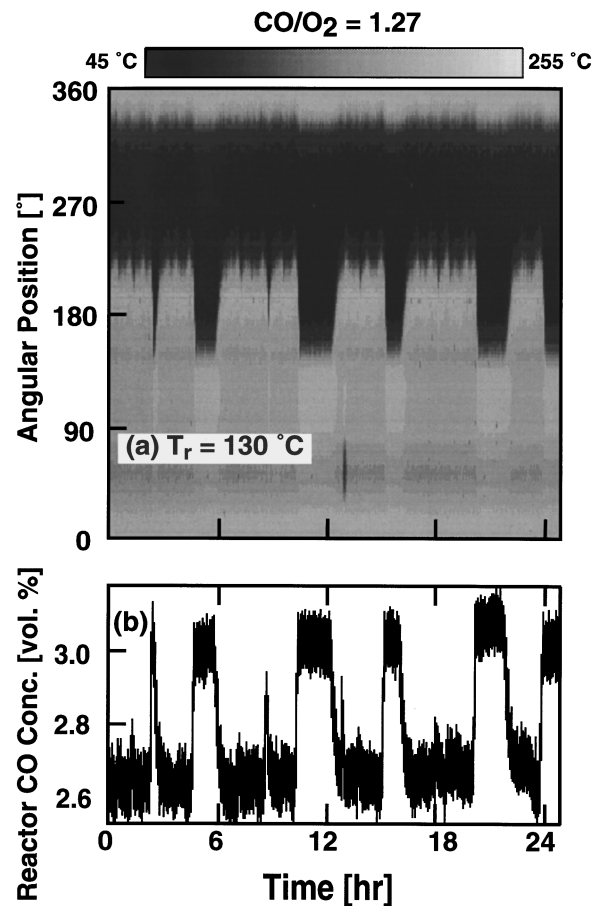


FIG. 7. Spatial relaxation oscillations of the temperature front for a feed containing 4 vol % CO and 3.16 vol % oxygen. (a) The surface temperature as a function of time and angular position. (b) Corresponding temporal effluent CO concentration (average CO conversion—30.7%).

gion(s) increased as the reactor temperature was decreased. This shifted the location of the fronts and affected their motion due to the catalyst nonuniformity. This is clearly illustrated by Figs. 4(c), 4(d), and 6.

For feeds containing 4 vol % CO, the shift from the stationary to the oscillating fronts occurred at a CO/O_2 concentration ratio of 1.85 (compared to 1.95 for a feed with 6 vol % CO). On another replica catalyst, for which the thermocouple sheaths did not contact the ring, the transition from stationary to oscillatory fronts also occurred with decreasing feed CO/O_2 concentration ratio. This indicates that the transition is generic for this catalytic system and does not depend on the nonuniformities.

In an experiment with a feed containing 4 vol % CO and a feed CO/O_2 ratio of 1.27, one of the fronts bounding the low temperature region exhibited irregular relaxation oscillations [Fig. 7(a)]. While the temperature front at 310° exhibited very low amplitude spatial movements, the other displayed large amplitude movements around 245° . This oscillatory behavior persisted for a few hours, then the front rapidly jumped to 160° and remained at that location for up to 2 h. It then relaxed back to 245° and remained there for several hours. The whole cycle was then repeated in an irregular fashion. The front sojourn at 245° was longer than at

160°. At times (2.4, 8.9 h), the front relaxed back to 245° almost immediately after reaching 160°. The ignition fronts moved at a lower velocity (0.5–1.1 mm/min) than the extinction fronts (1.6–2.6 mm/min). The effluent CO concentration oscillated in phase with the temperature fronts [Fig. 7(b)].

IV. DISCUSSION

The observed patterns illustrate the complex and rich dynamic features that can occur when an exothermic chemical reaction is carried out in the presence of both catalyst nonuniformity and global coupling. The intrinsic system nonuniformity and the local cooling generated by the touching thermocouple sheaths affected both the location and the dynamics of the temperature fronts. The global coupling, generated by the mixed reactants in the isothermal reactor, stabilized the nonuniform temperature patterns. For example, when a local high temperature region attempted to expand and conquer the surface, the increased overall reaction rate decreased the reactants concentration in the vessel. This, in turn, decreased the reaction rate everywhere on the catalytic ring, preventing further expansion of the high temperature region. For example, analysis of the temperature profiles of the case shown in Fig. 5(a) reveals a temperature decrease in the ignited region (around 180°) when it expanded at about 0.8–1.5 h after the experiment was started. In this bistable system, the ignited and extinguished regions were separated by temperature fronts which had a typical width of 4–5 mm. The temperature of the high temperature section of the catalyst increased as the reactor temperature decreased (Fig. 3) due to the increased reactant concentration in the vessel.

The rather similar motions which may be generated by either the global coupling or nonuniformity^{2,16,19} complicate the analysis due to ambiguity in deciding which effect generated a specific feature. We believe that in our experiments the nonuniformities had the dominant influence on the location and dynamics of the fronts, while the global coupling affected mainly the size of the high and low temperature regions. Stationary and moving fronts may be generated either by global coupling or nonuniformities. However, in the presence of global coupling, the stationary fronts may be placed at various locations on the ring by proper choice of the initial conditions, as observed by Somani *et al.*²⁶ during hydrogen oxidation on a supported nickel catalyst.

In our experiments the low temperature regions tended to form around the two locations (55° and 315°) in which increased heat loss occurred due to the touching of the ring by the thermocouple sheaths [Fig. 2]. The presence of two such locations enabled placing a low temperature region around either one or both locations [Figs. 3 and 4] by a proper choice of the initial conditions. The fact that the fronts preferred certain locations on the ring points out the strong influence of the nonuniformity. Similarly, the intricate motion of the temperature fronts shown in Figs. 4 and 6 must be due to the difference in the activity in the region around 230° from those around either 160° or 340°. The global coupling, on the other hand, most probably contributed to the synchronization of the back-and-forth motion of the two

fronts shown in Fig. 4(a). Similar interaction of nonuniformity and global coupling occurred, for example, in the experiments of Philippou *et al.*,⁵ in which a back-and-fourth motion was generated during the oxidation of propylene on a thin Pt wire kept at a constant average temperature by electrical heating. The motion occurred only on part of the ribbon, most probably due to the catalyst nonuniformity, while the global coupling by the electrical heating stabilized the moving front.

It is desirable to gain information about the nonuniformity of a system, such as ours, in which a direct measurement is not feasible. In a nonuniform bistable system, the front velocity varies with position, and the spatial variation of the observable variable usually reflects the nonuniformity of the system. Thus, in our system, the temperature of the fully ignited catalyst provides useful insight about the activity profile. Two approaches have been suggested for deducing the nonuniformity of experimental systems either from the front velocity^{12,15} or the time-averaged activator profile.¹⁶ Unfortunately, both approaches fail to provide useful results when the nonuniformity restricts the front motion to a fraction of the whole domain. For example, the average temperature profiles of Figs. 3(a) and 3(b) or Figs. 4(a) and 4(b) were rather different even though their nonuniformity was quite similar. Our experience suggests that the time-averaged profiles provide a good indication of the locations in which the activity is either high or low, but may fail to predict the relative activity.

Useful information about the front motion is also provided by the spatial profile of the standard deviation of the local temperature, i.e.,

$$\sigma(\phi) = \sqrt{\frac{\sum[T(t, \phi) - T_{\text{ave}}(\phi)]^2}{n-1}}, \quad (1)$$

where $T(t, \phi)$ and $T_{\text{ave}}(\phi)$ denote the temporal and time-averaged temperature at angular position ϕ , and n is the number of data points. The profile of $\sigma(\phi)$ provides information about the size of the region in which the fronts move back and forth. A wide (narrow) peak is indicative of spatial oscillations which occur over a wide (narrow) region and a shallow (sharp) activity profile. Figure 8 shows the profiles of $\sigma(\phi)$ of the four cases described in Fig. 4. The peaks in the profiles correspond to the oscillating temperature fronts. In all four cases the maximal $\sigma(\phi)$ of a pair of fronts strongly depended on the position on the ring. In general, the peak on the left-hand boundary is higher than that on the right-hand boundary. The location of the $\sigma(\phi)$ peaks of the two fronts bounding the low temperature region around 55° were rather similar for reactor temperatures of 140°, 130 and 120 °C, with a slight increase in the magnitude of the peak $\sigma(\phi)$ as the reactor temperature was decreased [Figs. 8(a), 8(c), and 8(d)]. The same was true for the two fronts bounding the cold region around 315° for reactor temperatures of 140 and 130 °C [Figs. 8(b) and 8(c)]. However, for a reactor temperature of 120 °C the front moved to 150°, causing a large decrease in the peak $\sigma(\phi)$ relative to its value at the higher

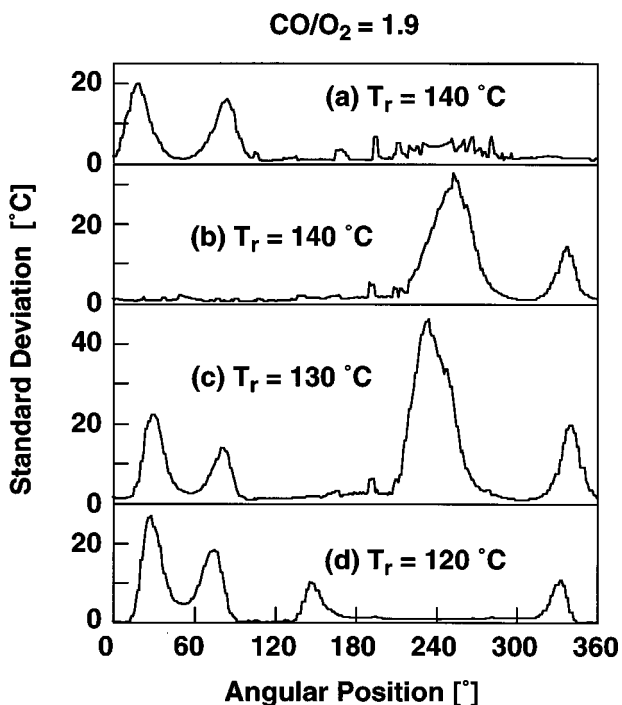


FIG. 8. Standard deviation of the local temperature vs angular position for the four cases shown in Fig. 4. The peaks correspond to the oscillating temperature fronts. The nonuniformity of the ring causes the difference in the spatial movements of the different fronts.

reactor temperatures [Fig. 8(d)]. The wider peak of $\sigma(\phi)$ around 240° in cases (b) and (c) suggests that the activity profile was shallower at that location.

The profiles of the standard deviation of the pattern shown in Fig. 6 during the first 3 h as well as during 4–8 h from the start of the experiment are shown in Fig. 9. In each of these two cases, the peak located in the 225° – 275° region

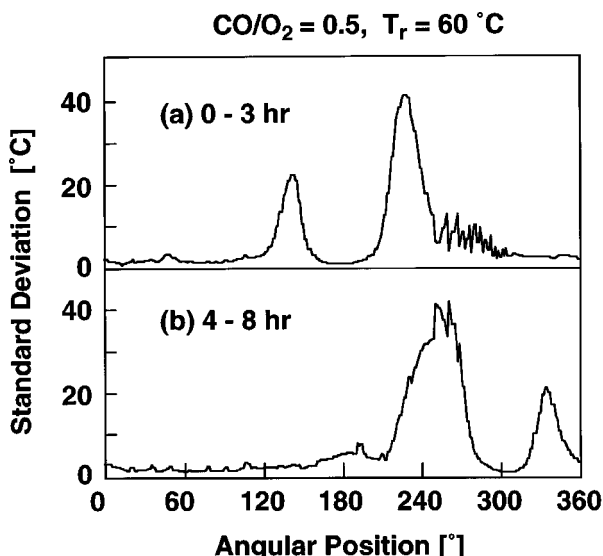


FIG. 9. Standard deviation of the local temperature vs angular position for the motion shown in Fig. 6. Profile (a) is for the first 3 h during which the low temperature region stayed around 155° and (b) is for the 4–8 h period in which the pulse stayed around 315° .

is about twice as high as that of the other boundary of the low temperature region. The maximal standard deviation in both cases is about equal.

The main advantages of the standard deviation plot are its clarity (as compared to, e.g., the time series of front location) and its sensitivity. Curve (d) in Fig. 8 may serve as an example. It indicates the existence of four moving fronts. The height of the four peaks correlates with the displacement amplitude. It also reflects the temperature variations in the region 140° – 200° that stem from the global coupling. It may also be noted that the cold region around 60° is so narrow that the moving fronts cause local temperature variations even at its very center, whereas the core temperature is constant for the broad cold spot around 300° . We feel that a plot of standard deviation of the observable variable versus position may also prove helpful in the description of two-dimensional patterns (e.g., straightforward detection of spiral tips, domain boundaries, inhomogeneities, etc.).

The transition from stationary to oscillatory fronts occurred for feed compositions with CO/O_2 concentration ratios of about 2. The fact that the transition occurred close to the composition of a stoichiometric mixture of the two reactants may be fortuitous. The observation of this transition at the same ratio for two different feed CO concentrations strongly suggests that this transition is affected mainly by the concentration ratio rather than the concentrations of the individual reactants. This transition is reminiscent of the pitchfork or Ising–Bloch bifurcation²² observed in a variety of other systems. The difference in the velocity of the ignition and extinction fronts suggests that the pitchfork was unfolded.

The ignition and extinction fronts shown in Fig. 4(a) moved at essentially the same velocity and direction, so that the low temperature region exhibited a back-and-forth motion. Theoretical analysis and simulations^{16,17,19} predict that such a motion may be generated in a nonuniform medium due to the reflection of a pulse, which would have rotated around the ring if it were a uniform medium. In most cases the motion of the two fronts bounding the low temperature region was out of phase, and the pulse motion resembles a breathing motion. In this work, the velocity of the extinction fronts exceeded that of the ignition fronts at the same location. A difference in the velocity of an ignition and extinction front at a given point was predicted for nonuniform systems described by the Fitzhugh–Nagumo model.^{14–17} Analyses and simulations in well-defined, nonuniform media suggest that front motion is strongly affected by the magnitude, slope, and length scale of the activity changes along the domain.^{16,21,29} Spatial changes with a length scale much smaller than the front width usually have only a minor impact on the front velocity.¹²

In our experiments, the differences in the asynchronous motions of the two fronts bounding the low temperature regions (Figs. 4–7) must have been due to the different activity at these two locations. Analysis of the motion in the Fitzhugh–Nagumo model by Hagberg *et al.*¹⁷ predicted that the spatial amplitude of the oscillatory motion of a front increases as the slope of the changing activity decreases. Our

experiments agree with this prediction as the amplitudes of the temperature oscillations of the fronts at 210° and 270° (Fig. 4) were much larger than those around 160° and 340°, while the slope of the temperature profile of the ignited states around 210° and 270° was much more moderate than next to 160° and 340° (Fig. 2).

V. CONCLUDING REMARKS

The experiments show that nonuniformities may lead to very intricate motions of temperature fronts on catalytic surfaces. Their presence may decrease the region of initial conditions leading to a specific state, i.e., increase the sensitivity of the system to the initial conditions. They point out the futility of any attempt to prepare a classification of all the possible patterns on such surfaces. Previous experiments had revealed either stationary or spatiotemporal patterns for a variety of atmospheric catalytic reactions. We believe that our study is the first to demonstrate the transition between these two types of motions in one system upon a change in the reactant composition. The data indicate that it would be useful to develop theoretical tools to discern the main features of the nonuniformity from the dynamics of the system. The activity of catalytic surfaces usually changes in the presence of atmospheric or high pressure reactions. Hence, any attempted potential application of temperature patterns to enhance the yield of a desired reaction would require knowledge of the impact of both intrinsic and induced nonuniformities, and development of robust and efficient control algorithms which can maintain a desired pattern in the presence of fluctuations and slowly evolving nonuniformities.

ACKNOWLEDGMENTS

This work was supported by grants from the National Science Foundation, the Welch Foundation, the Deutsche Forschungsgemeinschaft, NATO Grant No. CRG950142, and the Deutsche Akademische Austauschdienst. It is a pleasure to acknowledge helpful discussions with E. Meron, M. Bär, and M. Bode.

¹M. C. Cross and M. M. Hohenberg, Rev. Mod. Phys. **65**, 851 (1993); M. M. Slin'ko and N. I. Jaeger, *Oscillating Heterogeneous Catalytic Systems* (Elsevier, Amsterdam, 1994); A. Mikhailov, *Foundations of Synergetics, I: Distributed Active Systems*, 2nd ed. (Springer, Berlin, 1994); *Chemical Waves and Patterns*, edited by R. Kapral and K. Showalter (Kluwer, Dordrecht, 1994).

- ²U. Midya, D. Luss, and M. Sheintuch, J. Chem. Phys. **100**, 3568 (1994).
- ³W. Davies, Philos. Mag. **19**, 309 (1935).
- ⁴G. A. Cordonier and L. D. Schmidt, Chem. Eng. Sci. **44**, 1983 (1989); G. A. Cordonier, F. Schüth, and L. D. Schmidt, J. Chem. Phys. **91**, 5374 (1989); G. Philippou and D. Luss, Chem. Eng. Sci. **48**, 2313 (1993).
- ⁵G. Philippou, F. Schultz, and D. Luss, J. Phys. Chem. **95**, 3224 (1991).
- ⁶L. L. Lobban and D. Luss, J. Phys. Chem. **93**, 6530 (1989); S. L. Lane and D. Luss, Phys. Rev. Lett. **70**, 830 (1993); S. L. Lane, M. D. Graham, and D. Luss, AIChE J. **39**, 1497 (1993); S. Y. Yamamoto, C. M. Surko, M. B. Maple, and R. K. Pina, Phys. Rev. Lett. **74**, 4071 (1995); J. Chem. Phys. **102**, 8614 (1995).
- ⁷M. D. Graham, S. L. Lane, and D. Luss, J. Phys. Chem. **97**, 7564 (1993).
- ⁸M. Somaní, M. A. Liauw, and D. Luss, Chem. Eng. Sci. (to be published).
- ⁹J. C. Kellow and E. E. Wolf, Chem. Eng. Sci. **45**, 2597 (1990); AIChE J. **37**, 1844 (1991); F. Qin and E. E. Wolf, Chem. Eng. Sci. **49**, 4263 (1994); **50**, 117 (1995).
- ¹⁰G. Ertl, Science **254**, 1750 (1991); G. Ertl and R. Imbihl, Chem. Rev. **95**, 697 (1995); M. D. Graham, M. Bär, I. G. Kevrekidis, K. Asakura, J. Lauterbach, H.-H. Rotermund, and G. Ertl, Phys. Rev. E **52**, 76 (1995); K. C. Rose, D. Battogtokh, A. Mikhailov, R. Imbihl, W. Engel, and A. M. Bradshaw, Phys. Rev. Lett. **76**, 3582 (1996).
- ¹¹M. Bär, M. Hildebrand, M. Eiswirth, M. Falcke, H. Engel, and M. Neufeld, CHAOS **4**, 499 (1994).
- ¹²A. Kulka, M. Bode, and H.-G. Purwins, Phys. Lett. A **203**, 33 (1995).
- ¹³G. Haas, M. Bär, I. G. Kevrekidis, P. B. Rasmussen, H.-H. Rotermund, and G. Ertl, Phys. Rev. Lett. **75**, 3560 (1995).
- ¹⁴P. Schütz, M. Bode, and H.-G. Purwins, Physica D **82**, 382 (1995).
- ¹⁵M. Bode and H.-G. Purwins, Physica D **86**, 53 (1995).
- ¹⁶M. A. Liauw, J. Ning, and D. Luss, J. Chem. Phys. **104**, 5657 (1996).
- ¹⁷A. Hagberg, E. Meron, I. Rubinstein, and B. Zaltzman, Phys. Rev. Lett. **76**, 427 (1996).
- ¹⁸A. K. Bangia, M. Bär, I. G. Kevrekidis, M. D. Graham, H.-H. Rotermund, and G. Ertl, Chem. Eng. Sci. **51**, 1757 (1996).
- ¹⁹M. Sheintuch, J. Phys. Chem. **100**, 15137 (1996).
- ²⁰M. Bär, A. K. Bangia, I. G. Kevrekidis, G. Haas, H.-H. Rotermund, and G. Ertl, J. Phys. Chem. **100**, 19106 (1996).
- ²¹S. Shvartsman, A. K. Bangia, M. Bär, and I. G. Kevrekidis, in *Disordered Media*, IMA volume on Mathematics and its Applications, edited by K. Golden, G. Grimmett, G. Milton, and P. Sen (to be published).
- ²²P. Coullet, J. Lega, and Y. Pomeau, Europhys. Lett. **15**, 221 (1991); A. Hagberg and E. Meron, Nonlinearity **7**, 805 (1994); J. Rinzel and D. Terman, SIAM J. Appl. Math. **42**, 1111 (1982).
- ²³M. Bode, A. Reuter, R. Schmeling, and H.-G. Purwins, Phys. Lett. A **185**, 70 (1994).
- ²⁴K. J. Lee, W. D. McCormick, H. I. Swinney, and J. E. Pearson, Nature (London) **369**, 215 (1994); K. J. Lee and H. L. Swinney, Phys. Rev. E **51**, 1899 (1995).
- ²⁵M. Somaní, Ph.D. dissertation, University of Houston, 1996.
- ²⁶M. Somaní, M. A. Liauw, and D. Luss, Chem. Eng. Sci. **51**, 4259 (1996).
- ²⁷D. T. Lynch and S. E. Wanke, J. Catal. **88**, 333 (1984); M. Sheintuch and J. Schmidt, J. Phys. Chem. **92**, 3404 (1988).
- ²⁸M. A. Liauw, M. Somaní, J. Annamalai, and D. Luss, AIChE J. **43**, 1519 (1997).
- ²⁹K. Agladze, R. R. Aliev, T. Yamaguchi, and K. Yoshikawa, J. Phys. Chem. **100**, 13895 (1996).